Asymmetric Squares as Standing Waves in Rayleigh-Bénard Convection

Alaka Das, Ujjal Ghosal and Krishna Kumar

Physics and Applied Mathematics Unit, Indian Statistical Institute

203, Barrackpore Trunk Road, Calcutta-700 035, India

Abstract

Possibility of asymmetric square convection is investigated numerically using a few mode Lorenz-like model for thermal convection in Boussinesq fluids confined between stress free and conducting flat boundaries. For relatively large value of Rayleigh number, the stationary rolls become unstable and asymmetric squares appear as standing waves at the onset of secondary instability. Asymmetric squares, two dimensional rolls and again asymmetric squares with their corners shifted by half a wavelength form a stable limit cycle.

PACS numbers: 47.20.Ky, 47.27.-i

Two dimensional stationary roll-patterns are known to be the only stable solutions at the onset of thermal convection in a thin layer of Boussinesq fluid confined between conducting boundaries[1] except in the case of fluids with vanishingly small Prandtl number[2]. The stationary convection in the form symmetric square cells are unstable [1] except in fluids of very high Prandtl number σ at very high values of Rayleigh number R [3]. Assenheimer and Steinberg[4] observed an interesting possibility of hexagonal convective cells with both up- and down- flow in the center of the cell at R approximately twice the value of critical Rayleigh number R_c. The possibility of dual types of hexagonal convective cells was also established by Clever and Busse [5]. Recently, Busse and Clever[6] predicted a new possibility of stationary convection in the form of asymmetric square cells with both up- and down- flow in the center for rigid and thermally conducting horizontal boundaries.

In this work we construct and study a Lorenz-like model[7] that describes convection patterns in the form of rolls and squares, both symmetric as well as asymmetric ones, in a thin layer of Boussinesq fluid of moderate and high Prandtl numbers ($\sigma > 2$) at high values of R. The nonlinear superposition of mutually perpendicular sets of rolls of the same wave number would be called asymmetric squares when the structure (e.g., shadowgraph picture) does not possess four-fold symmetry. It happens when the intensities of the two set of rolls are different. The model allows us to study competetion between rolls and asymmetric squares. In the following we shall derive the model from hydrodynamic equations and investigate the model numerically for possible stable solutions. We then present the results and discuss them.

We consider an infinite layer of Boussinesq fluid of kinematic viscosity ν, thermal diffusitivity κ and thickness d confined between two perfectly conducting horizontal boundaries and heated underneath. Using the length scale d, the time scale $\frac{d^2}{\kappa}$, and the temperature scale as the temperature difference ΔT between lower and upper boundaries, the non-dimensional form of hydrodynamic equations in Boussinesq approximation read

$$\partial_t \mathbf{v} + (\mathbf{v}.\nabla)\mathbf{v} = -\nabla p + \sigma(\theta \mathbf{e_3} + \nabla^2 \mathbf{v}) \tag{1}$$

$$\nabla.\mathbf{v} = 0 \tag{2}$$

$$\partial_t \theta + \mathbf{v}.\nabla\theta = \nabla^2\theta + R\mathbf{v}.\mathbf{e_3} \tag{3}$$

where $\mathbf{v} = (v_1, v_2, v_3)$ are the velocity fields, θ the deviation from the conductive temperature profile and p the deviation from static pressure of conductive state due to convective instability. Prandtl number σ and Rayleigh number R are defined as $\sigma = \frac{\nu}{\kappa}$ and $R = \frac{\alpha(\Delta T)gd^3}{\nu\kappa}$, where α is the coefficient of thermal expansion of the fluid, g the acceleration due to gravity. The unit vector $\mathbf{e_3}$ is directed vertically upward, which is assumed to be the positive direction of x_3-axis. The boundary conditions at the stress-free conducting flat surfaces imply $\theta = v_3 = \partial_{33}v_3 = 0$ at x_3=0, 1. Taking curl twice of the momentum equation (Eq. 1) and using the continuity condition (Eq. 2), the equation for vertical velocity reads

$$\partial_t \nabla^2 v_3 = \sigma\nabla^4 v_3 + \sigma\nabla_H{}^2\theta - \mathbf{e_3}.\nabla \times [(\omega.\nabla)\mathbf{v} - (\mathbf{v}.\nabla)\omega] \tag{4}$$

where $\omega = \nabla \times \mathbf{v}$ is the vorticity, and $\nabla_H{}^2 = \partial_{11} + \partial_{22}$ is the horizontal Laplacian.

We employ the standard Galerkin procedure to describe the convection patterns at the onset of secondary instability in relatively high Prandtl number fluids. The spatial dependence of all vertical velocity and temperature field are expanded in a Fourier series, which is compatible with the stress-free flat conducting boundaries and periodic boundary conditions in the horizontal plane. Here, we restrict ourselves to standing patterns and, hence all time-dependent fourier amplitudes will be assumed to be real. The expansions for all the fields are truncated to describe straight cylindrical rolls and patterns arising from the nonlinear superposition of mutually perpendicular set of rolls of the same wavenumber. Perturbative fields with the same wavelength in mutually perpendicular directions are likely to occur in square containers. The vertical velocity v_3 and θ then read as

$$v_3 = [W_{101}(t)cos(kx_1) + W_{011}(t)cos(kx_2)]sin(\pi x_3) + W_{112}(t)cos(kx_1)cos(kx_2)sin(2\pi x_3)$$

$$+ ..., \tag{5}$$

$$\theta = [\Theta_{101}(t)cos(kx_1) + \Theta_{011}(t)cos(kx_2)]sin(\pi x_3) + \Theta_{112}(t)cos(kx_1)cos(kx_2)sin(2\pi x_3)$$

$$+ \Theta_{002}(t)sin(2\pi x_3) + ... \tag{6}$$

The horizontal components of the velocity field can easily be computed using the equation of continuity. Projecting Eq.(4) for v_3 and the equation for θ (Eq. 3) on above modes, we arrive at the following minimal mode Lorenz-like model

$$\tau \dot{\mathbf{X}} = \sigma(-\hat{q}^2\mathbf{X} + \frac{\hat{k}^2}{\hat{q}^2}\mathbf{Y}) + \begin{pmatrix} X_2 \\ X_1 \end{pmatrix} S \tag{7}$$

$$\tau \dot{\mathbf{Y}} = -\hat{q}^2\mathbf{Y} + (r - Z)\mathbf{X} + \begin{pmatrix} X_2 \\ X_1 \end{pmatrix} T \tag{8}$$

$$\tau \dot{S} = -2\sigma\hat{d}^2 S + \sigma\frac{\hat{k}^2}{\hat{d}^2}T - \frac{\hat{q}^2}{2\hat{d}^2}X_1 X_2 \tag{9}$$

$$\tau \dot{T} = -2\hat{d}^2 T + rS - \frac{1}{4}(X_1 Y_2 + X_2 Y_1) \tag{10}$$

$$\tau \dot{Z} = -bZ + \mathbf{X}.\mathbf{Y} \tag{11}$$

3

where the linear modes $\mathbf{X} = \begin{pmatrix} X_1 \\ X_2 \end{pmatrix} = \frac{\pi}{\sqrt{2}q_c^2} \begin{pmatrix} W_{101} \\ W_{011} \end{pmatrix}$ and $\mathbf{Y} = \begin{pmatrix} Y_1 \\ Y_2 \end{pmatrix} = \frac{k_c^2}{2\sqrt{2}q_c^5} \begin{pmatrix} \Theta_{101} \\ \Theta_{011} \end{pmatrix}$ represent the vertical velocity and the temperature field respectively. The nonlinear mode $Z = \frac{-\pi k_c^2}{q_c^6}\Theta_{002}$ denotes heat flux across the fluid layer. Modes $S = \frac{\pi}{4q_c^2}W_{112}$ and $T = \frac{\pi k_c^2}{4q_c^6}\Theta_{112}$ are essential to describe nonlinear coupling between two sets of mutually perpendicular rolls. The parameters defined by $k^2 = \pi^2 + k^2$, $\hat{q}^2 = \frac{q^2}{q_c^2}$, $\hat{k}^2 = \frac{k^2}{k_c^2}$, $\hat{d}^2 = \frac{2\pi^2+k^2}{q_c^2}$ are, in general, wavenumber dependent, while other parameters given by $k_c^2 = \frac{\pi^2}{2}$, $q_c^2 = \pi^2 + k_c^2$, $\tau = \frac{1}{q_c^2}$, $b = \frac{4\pi^2}{q_c^2}$ are constants in the model. The reduced Rayleigh number $r = \frac{Rk_c^2}{q_c^6}$ is the control parameter of the problem. We set, hereafter, $k = k_c$, the wavenumber of stationary rolls at the onset of primary instability. This makes $\hat{k}^2 = \hat{q}^2 = 1$, $\hat{d}^2 = \frac{5}{3}$ and $b = \frac{8}{3}$ in our model for convection.

The steady two dimensional(2D) rolls parallel to x_1-axis is given by $X_1 = 0 = Y_1$. This makes the nonlinear modes S and T to decouple from the system. Our model then reduces to well known Lorenz model with steady solutions given by $X_2 = Y_2 = \sqrt{b(r-1)}$ and $Z = r-1$. However, these solutions become unstable at much lower values of reduced Rayleigh number r than that predicted by the original Lorenz model[7]. The lower curve in the Figure 1 shows the critical value r_o of reduced Rayleigh number, at which the 2D rolls become unstable, as a function of the Prandtl number σ. The critical value r_o increases with increasing σ.

The steady and perfect squares are obtained by setting $X_1^2 = X_2^2$ in our model. Such solutions are given by,

$Y_2^2 = Y_1^2$, $\quad Y_1 = -\frac{2\sigma(r-4\hat{d}^6)rX_1+rX_1^3}{2\sigma\hat{d}^4X_1^2 - 2\sigma(r-4\hat{d}^6)(1+\frac{2X_1^2}{b})}$, $\quad S = \frac{sign(X_1X_2)}{\sigma(r-4\hat{d}^6)}(\frac{\sigma}{4}\mathbf{X}.\mathbf{Y} + \hat{d}^2X_1^2)$,

$T = \frac{sign(X_1X_2)}{2\sigma(r-4\hat{d}^6)}(\sigma\hat{d}^4\mathbf{X}.\mathbf{Y} + rX_1^2)$, $\quad Z = \frac{1}{b}(\mathbf{X}.\mathbf{Y})$, where X_1 is a possible real root of the algebraic equation

$X_1^4 + AX_1^2 + B = 0$

with $A = \frac{2\sigma^2\hat{d}^4 - \frac{4\sigma^2}{b}+2\hat{d}^2+2\sigma r}{(\frac{4\hat{d}^2}{b}+\frac{1}{2})}$ and $B = \frac{2\sigma^2(r-4\hat{d}^6)(r-1)}{(\frac{4\hat{d}^2}{b}+\frac{1}{2})}$. For $1 < r < r_o(= 4\hat{d}^6)$, which defines the validity range of the model, B is negative and consequently positive root of X_1^2 exists. This implies that the convective patterns in the form of perfect squares exist. However,

4

they are found to be always unstable.

We study the time-dependent solutions by numerically integrating our model. We investigate the dynamics of the patterns as a function of increasing r in two ways- first by using the data from previous solution as initial conditions for a new r; and secondly by choosing randomly small values of all variables as initial conditions. We get the same result with suitably chosen initial conditions. For $r_o < r < r_{ir}$ (see Fig. 1), we find oscillatory solutions. The stationary rolls become unstable and a new set of rolls perpendicular of the old one develops. The competition between these two sets of rolls leads to a time periodic sequence of rolls and patterns arising from nonlinear superposition of two sets of rolls. For $r \geq r_{ir}$, the solutions become irregular in time indicatiing more modes are required to study this regime of parameter space.

Figure 2 shows the temporal behaviour of the amplitude X_1 of the new set of rolls as well as the amplitude X_2 of the old set of rolls. While X_1 oscillates with zero mean, X_2 oscillates around a finite value. The time period of X_1 is always double of that of X_2. In fact all the modes (X_1, Y_1, S, T) that develop at $r > r_o$ oscillate with same period and with zero mean. The periods of Y_2 and Z are the same as that of X_2. The frequency $f = 1/T$ of oscillation of X_2 at the onset of oscillatory instability increases with increasing Prandtl number (see Fig. 3).

The projection of limit cycle on $Y_1 - Y_2$ plane is shown in Fig. 4. The mean of oscillating amplitude of 2D roll mode (Y_2) decreases and the perturbative amplitude (Y_1) increases with increasing r. Figure 5 shows the sequence of shadowgraphs of the patterns for $r_o < r < r_{ir}$. The intensity of old 2D rolls decreases when a new set of rolls perpendicular to the old one appears. While the spatial positions for up and down flows in the old set remain fixed, these positions alternate for new set of rolls. Consequently, the corner positions of square patterns slide back and forth along the set of old rolls. The standing waves in form of square patterns do not have four-fold symmetry although they preserve inversion symmetry. The time periodic appearances of asymmetric squares, 2D rolls, asymmetric squares again with shifted positions of the maximum up or down flows by half a wavelength and 2D rolls form a limit cycle. Although the competetion between

5

rolls and symmetric squares is known in binary mixtures[8, 9], but time periodic sequence of asymmetric squares and two dimensional rolls in pure fluids is qualitatively new.

We now test the stability of this limit cycle by introducing the vertical vorticity in the model. We expand the vertical vorticity ω_3 as

$$\omega_3 = [\zeta_{101}(t)cos(kx_1) + \zeta_{011}(t)cos(kx_2)]cos(\pi x_3) + \zeta_{110}(t)cos(kx_1)cos(kx_2)$$

$$+ \ ..., \tag{12}$$

Simultaneously, for the consistency of the model, we add a mode $W_{\bar{1}\bar{1}2}$ in the expansion of vertical velocity v_3, and a similar mode $\Theta_{\bar{1}\bar{1}2}$ in the expansion of temperature field θ. This makes a Lorenz-like model consisting of twelve modes. The results of this model for fluids with $\sigma > 2$ exactly reproduces the results of the seven mode model discussed earlier. Only for $\sigma < 2$ and much higher values or r, vertical vorticity is excited. So for $\sigma > 2$ and perturbations of wavenumber same as that of 2D rolls, we always see a stable limit cycle. The results of our model indicate that for fluids with moderate and large values of Prandtl number enclosed preferably in a square container, the time periodic competition between the asymmetric squares and rolls should be realizable.

FIGURES

Figure 1. The region of r and σ space showing space rolls, asymmetric squares and irregular solutions. The lower curve shows the values of reduced Rayleigh number r_o above 2D rolls become unstable and time periodic asymmetric squares appear. The upper curve corresponds to the onset of irregular solutions in the model.

Figure 2. The convective amplitudes X_1 and X_2 of new and old sets of rolls respectively with respect to time for $r = 14.5$ and $r = 14.7$ with value of $\sigma = 10$. The time period of the new set of rolls is always double that for the old set of rolls, which became stable.

Figure 3. The plot of the frequency $f = 1/T$ of the amplitude X_2 as a function of Prandtl number σ at the onset of secondary instability.

Figure 4. The projection of limit cycle on $Y_1 - Y_2$ plane for different values of r for $\sigma = 10$. Upper and lower plots correspond to $r = 14.5$ and $r = 14.7$ respectively. The mean of 2D roll mode (Y_2) decreases and the perturbative amplitude Y_1 increases with increasing r.

Figure 5. Time-periodic sequence of asymmetric squares and rolls in shadowgraph for $r = 14.7$ and $\sigma = 10$. Shadowgraphs a,b,c correspond respectively to maximum, zero and minimum values of Y_1 in Fig. 4.

REFERENCES

1. Schlüter, A., Lortz, D. and Busse, F., *J. Fluid Mech.* **23**, 129 (1965).

2. Thual, O., *J. Fluid Mech.* **240**, 229 (1992); see also Kumar, K., Fauve, S. and Thual, O., *J. Phys. II France* **6**, 945 (1996).

3. Whitehead, J. A. and Parsons, B., *Geophys. Astrophys. Fluid Dyn.* **9**, 201 (1978).

4. Assenheimer, M. and Steinberg, V., *Phys. Rev. Lett.* **76**, 756 (1996).

5. Clever, R. M. and Busse, F. H., *Phys. Rev. E* **53**, R2037 (1996).

6. Busse, F. H. and Clever, R. M., *Phys. Rev. Lett.* **13**, 341(1998).

7. Lorenz, E. N., *J. Atmos. Sci.* **20**, 130 (1963).

8. Moses, E. and Steinberg, V. *Phys. Rev. Lett.* **57**, 2018 (1986).

9. Müller, H. W. and Lücke, M. *Phys. Rev. A* **38**, 2965 (1988).
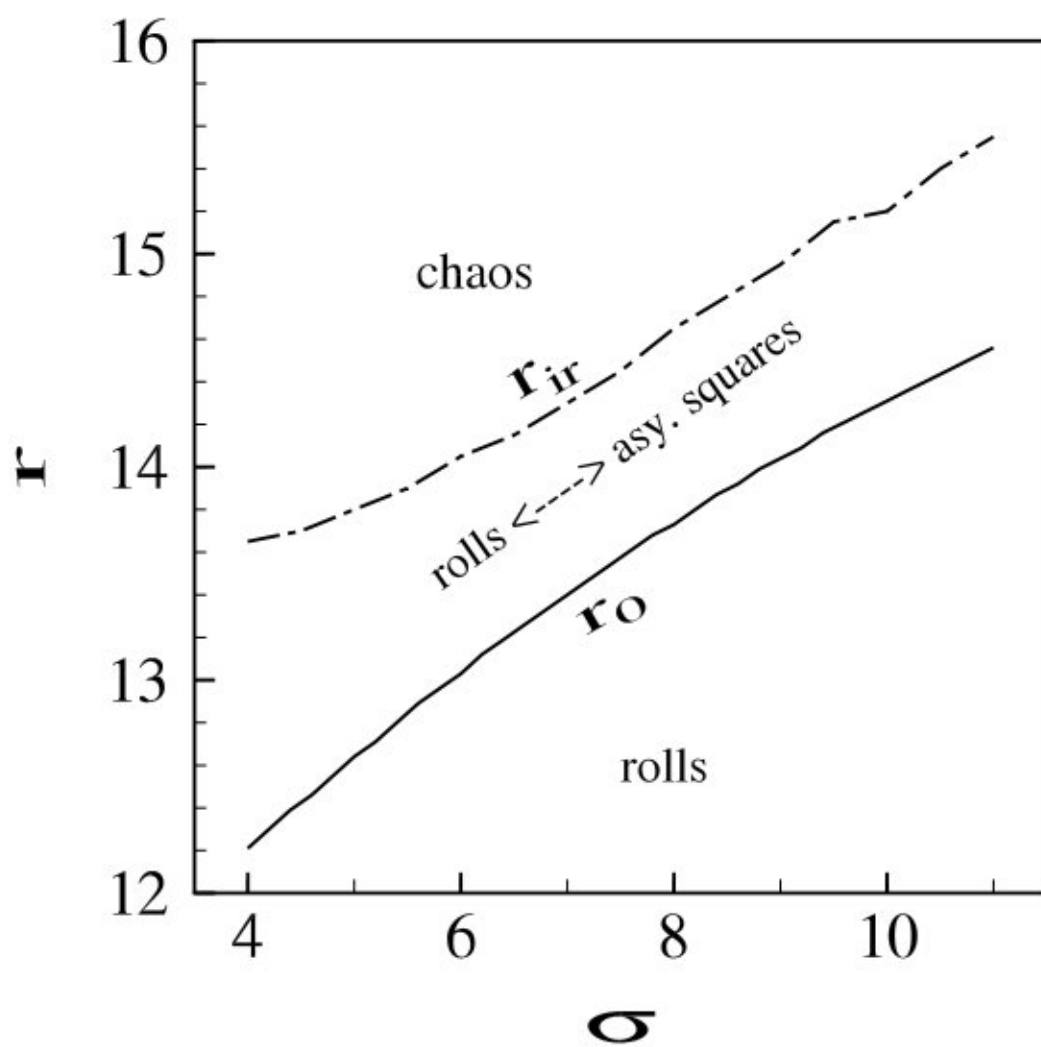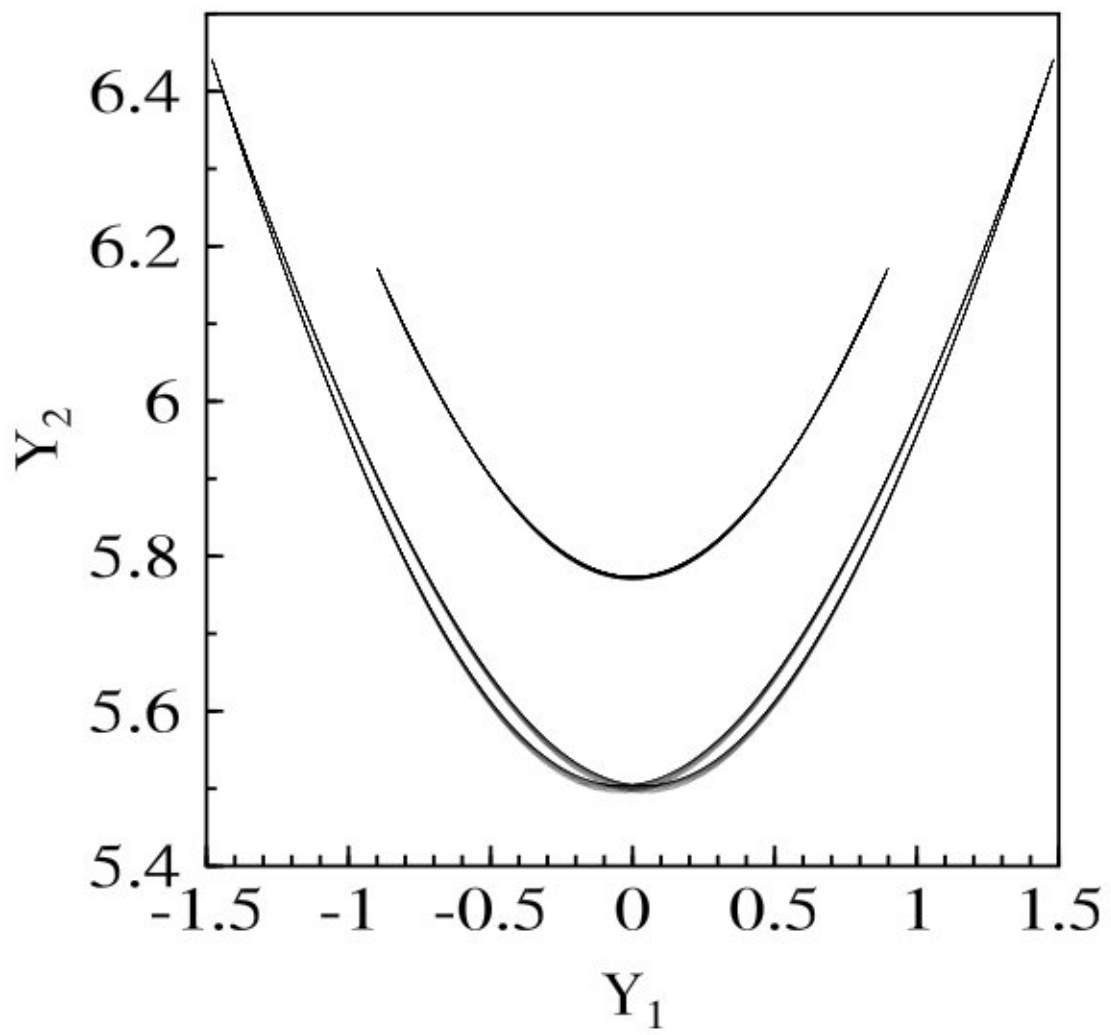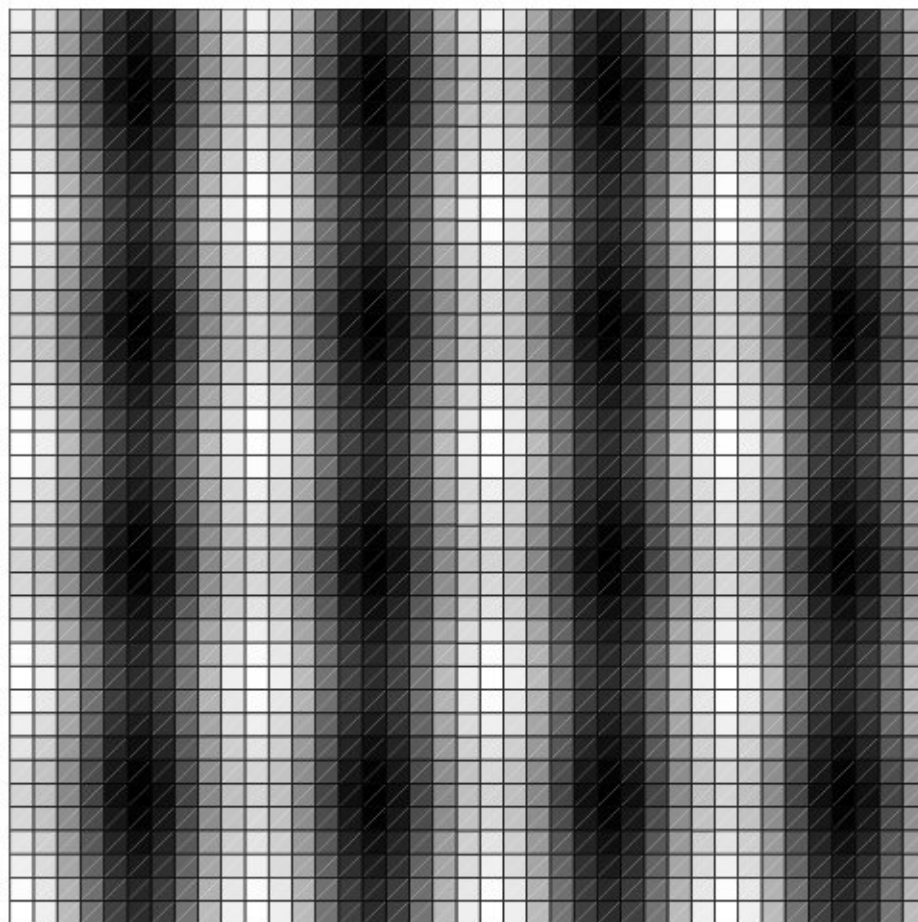
FIGURE 1
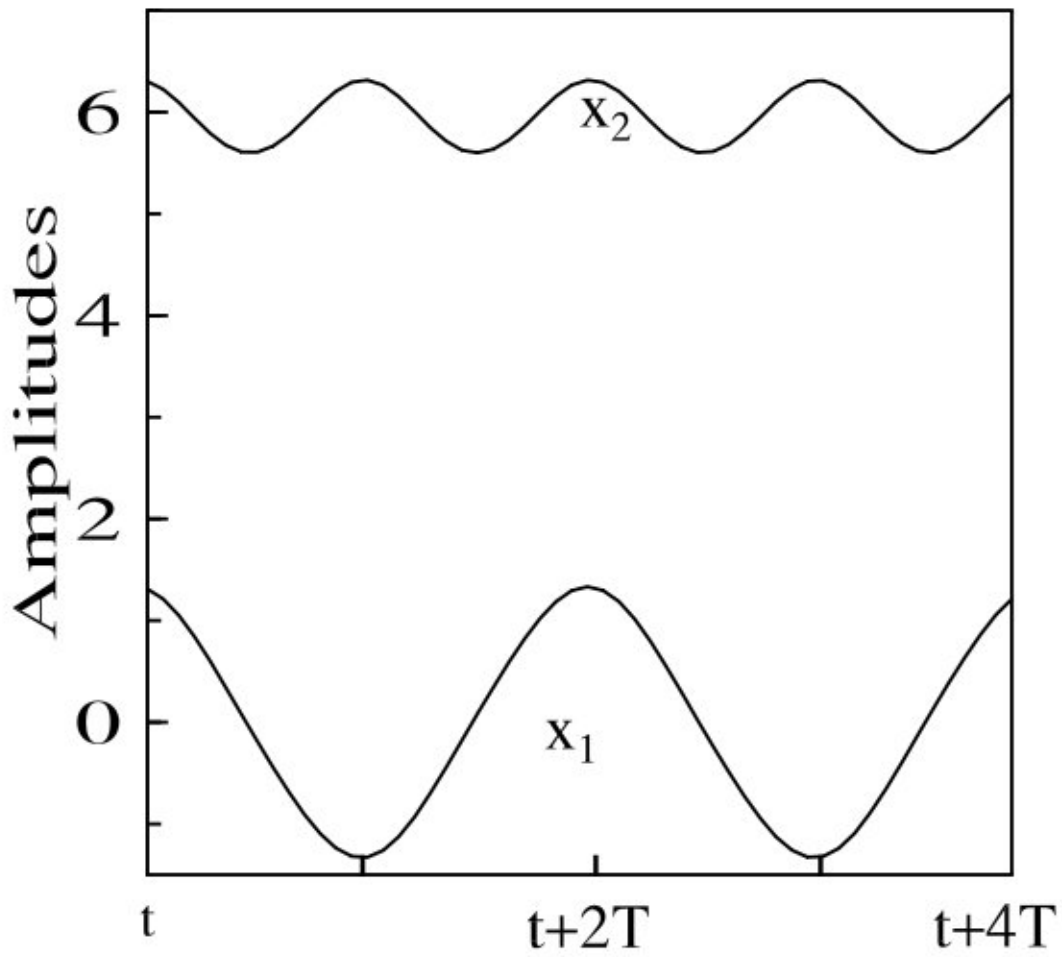
FIGURE 2
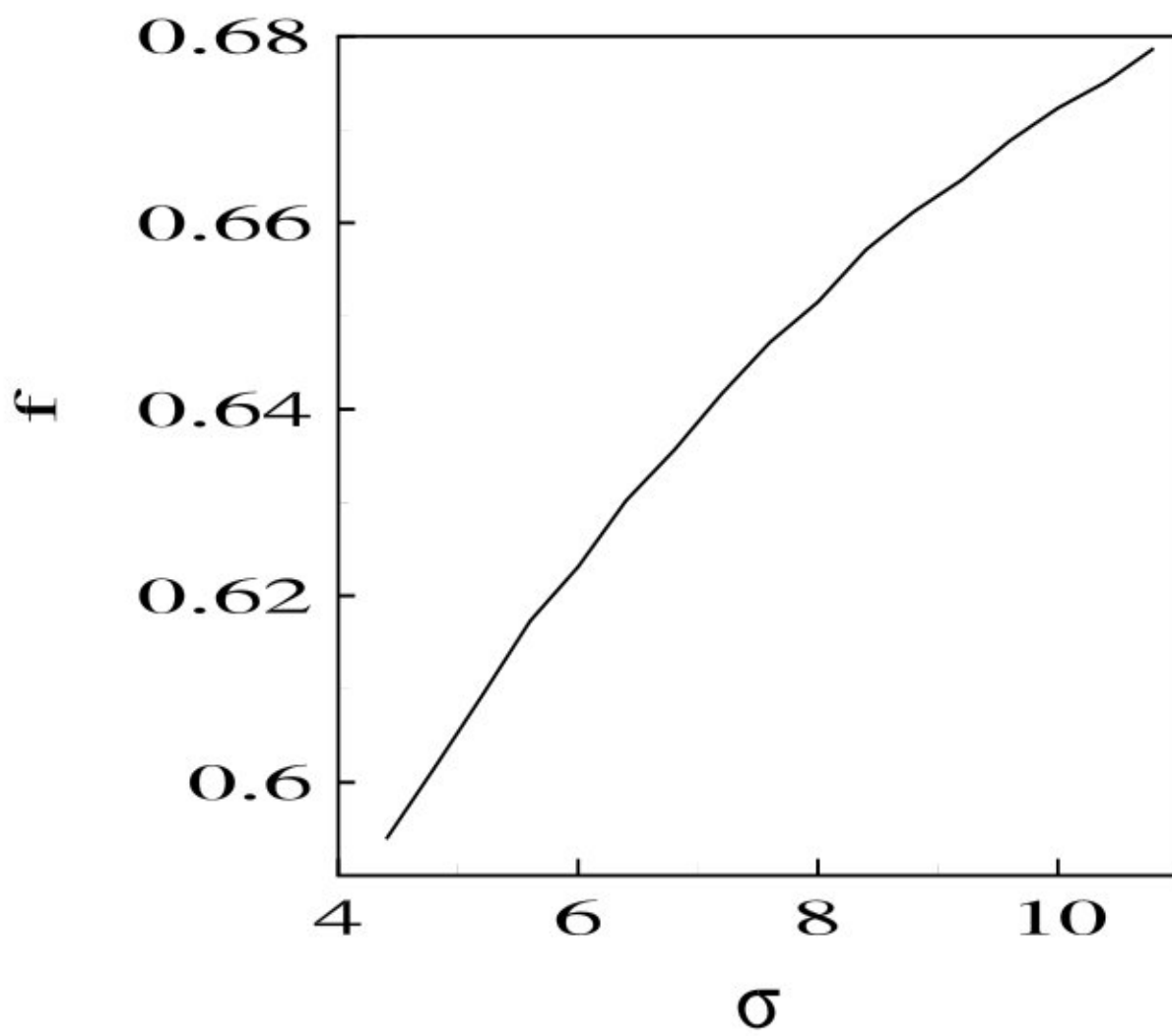
FIGURE 3

FIGURE 4

FIGURE 5a

FIGURE 5b

FIGURE 5c